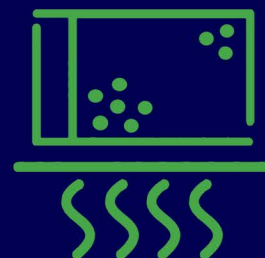




# FOAMS<sup>®</sup> 2021

September 13-16, 2021 • Virtual Conference  
Presented by SPE Thermoplastic Materials & Foams Division



# Conference Proceedings

# DESIGN OF MICROFOAMED STRANDS AND HIERARCHICALLY STRUCTURED OBJECTS BY CONTINUOUS 3D FOAM PRINTING

*Daniele Tamaro, Massimiliano Maria Villone and Pier Luca Maffettone,  
University of Naples Federico II, Dipartimento di Ingegneria Chimica, dei Materiali e della  
Produzione Industriale, Naples, IT*

## Abstract

We report the design and the results of a novel process that combines 3D printing and foaming to produce microfoamed polymeric structures, from strands to more complex architectures, using physical blowing agents. In the context of polymeric cellular materials, foaming processes, either using physical or chemical blowing agents, are extensively operated in industry to produce pores, yet without a spatial control of the pore positioning. This intrinsic stochastic structuring may introduce imperfections, which reduce the overall mechanical properties of the material; thus, regular (e.g., periodic) structures are more desirable than stochastic ones. 3D printing is another technique to fabricate polymeric cellular materials and it allows to produce cellular materials with empty spaces in precise locations and with a well-defined periodic structure. To this end, very expensive 3D printers are required to achieve micron-resolution pores. Correspondingly, the production time increases dramatically, and becomes a bottleneck to the industrial scale-up. Herein, we present an innovative technique that combines the simplicity of polymer foaming with the precision of 3D printing. The resulting cellular materials have the advantages of both techniques: they have a micron-controlled cell structure and can be printed at reasonable costs and time. The proposed approach is validated using a biobased and compostable polymer for application in biomedical, agriculture and chemical engineering fields. The resulting foamed strands are novel in terms of morphology with a controlled local porosity that opens up to an immense scenario of applications thanks to a possible cost-effective production of hierarchical structures with superior properties (e.g., scaffolds for bioengineering and advanced devices for energy storage or collection).

## Introduction

3D printing has been revolutionizing the way to transform materials into functional 3D objects by virtue of a) an incredible freedom of design compared to traditional techniques, b) a high sustainability due to waste minimization, c) the possibility of mass customization because, for small number of items, it is more economical than other traditional techniques [1]. The number of

applications is quickly raising in a wide range of industries, for instance in automotive for moquette and prototypes, in medicine for medical implants and scaffolds, and in construction industry as a core method to fabricate buildings or components [2] [3] [4]. Among the numerous techniques for 3D printing, we here present an innovative version of Fused Deposition Modelling (FDM) for printing foams. The FDM is a method that uses a continuous filament of a thermoplastic polymer to 3D print layers of materials. The filament is heated at the nozzle of the printer and extruded through a small orifice on a platform or on top of previously printed layers. Our novel technique, which could be defined 3D foam printing, produces microfoamed strands and/or structures by inline impregnation of physical blowing agent in the filament that will foam at the nozzle exit. In passing, in what follows we define filaments to refer to polymer fed to the printer, and strands to refer to foamed polymer exiting the nozzle.

Foams are widely applied in several technological fields, offering distinctive characteristics that derive from their special internal porous morphology [5] [6] [7] [8]. The characteristic size of the pores, their shape, and their hierarchical organization are important factors in determining the structure–property relationship in these materials [9]. It is known that hierarchical porous structures outperform their nonhierarchical counterparts in regards of mechanical behavior (i.e., superior mechanical robustness and energy absorption performance for honeycomb and cellular lattice) and accessible active surface [6][10]. As matter of fact, nature has often chosen optimized hierarchical structures to shape lives on our planet [11]. 3D printing of foamed hierarchical structures, which is appealing in several industrial fields, is still challenging due to the difficulty of forming internal micro-porous structure with the existing printing techniques. Efforts have been made to print polymers into cellular or mesh structures by piling up extruded strands, where macroscale pores are generated by the computer-designed spacing between the filamentary struts. Nevertheless, the extruded strands are still densely packed, and porous structure is directly restricted by the printing resolution, which results in low porosity limited to the external strand surface; moreover, the printing time increases as the cost to pay for high resolutions [12]. Many attempts have been made to produce 3D printed foams with high porosity and internal-

strand micro-pores. The current solutions are based on two-stage approaches that consist in a first step where structures with inter-strands macro-porosity are printed and a second step where the intra-strand micro-porosity is produced by freeze-drying [13] or batch foaming [14]. Recently, a solution has been proposed where the first step consists of preparing either an emulsion [15] or a treated filament [16], which, in the second step, is heated up through a 3D printer to produce the final foamed strand. Such approaches suffer the complexities of multi-stage processes and are seldom capable of fine control of the foamed strand morphologies. Hence, less expensive and less time-consuming alternative methods that could address these limitations and cover a wide range of controlled pore size, porosity, and pore morphology are highly demanded to enable full exploitation of the rich design space offered by hierarchical structures.

We here propose a simple and cost/time-effective 3D printing technique to produce microfoamed strands in only one step. We achieve a fine tuning of cell morphology in the printed strands by designing the operating conditions through the modelling of transport phenomena. We report the results of an extensive experimental campaign for the production of micro-foamed strands with a controlled density and morphology. Model-based design of the operating conditions result in the formation of structures with a wide range of pore sizes (from 10 to 500 microns) and densities. The proposed approach opens up to a broad scenario of opportunities to optimize mechanical, thermal, and electrical properties of 3D printed structures. Noteworthy, our approach is here applied with use of biodegradable and biobased polymer, thus allowing for a sustainable production.

## Materials and Methods

### Materials

Poly(lactic acid) (PLA), grade NW2003D from NatureWorksLLC, was used in this study. PLA pellets were dried overnight at 60°C in oven under vacuum conditions before any manipulation. A PLA filament with diameter of 1.75 mm was produced using a Composer350 extruder (from 3DEVO company, The Netherlands), whose process parameters are given in Table 1. A Prusa Research I3 Mk3s 3D printer was then used to foam the filament. The blowing agent, acetone, was supplied by Sigma Aldrich (Germany).

Table 1: Filament extrusion process conditions.

Screw speed	Zone 1 (feeding)	Zone 2 (melting)	Zone 3 (mixing)	Zone 4 (shaping)	Fan speed
5.0 rpm	150 °C	180 °C	200 °C	190 °C	500 rpm

The foams were characterized to determine their bulk density ( $\rho$ ) and cell density ( $N$ ).  $\rho$  was measured according to ASTM D7710, using an analytical balance (Mettler Toledo, Columbus, OH). The samples were first sectioned with a razor blade in liquid nitrogen and then coated with gold using a sputter coater. The cellular structure of the foams was investigated by using a scanning electron microscope (Hitachi TM 3000 SEM).

## Results

### The novel 3D foam printing

In order to end up with a single-stage strand foaming during printing, one needs the following processes to be completed in series: 1) solubilization of the blowing agent in the filament to be foamed, 2) modification of the concentration profile of the blowing agent in the filament, 3) foaming at the exit of the printer nozzle, 4) stabilization of the foamed filament, 5) deposition of the foamed filament. Thus, the proposed technology can be schematized with the following units (see Figure 1): a) solubilization of the blowing agent into the filament, b) desorption of the blowing agent, c) melting, d) foaming, and e) adhesion of the strands.

Mass transport phenomena in the first two units are modelled to achieve specific foam morphologies in the foamed strand.

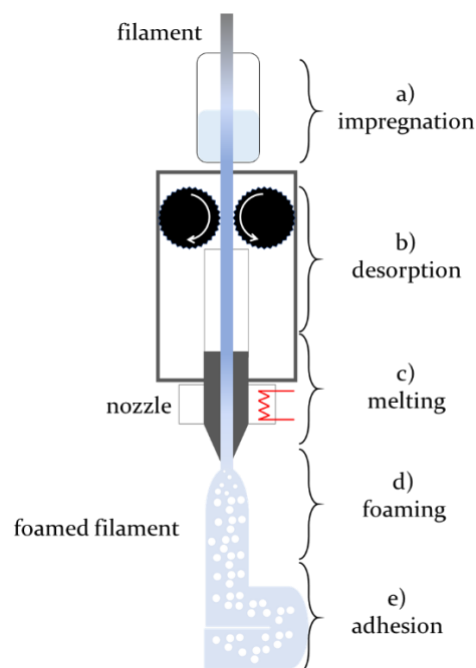


Figure 1: Sketch of the 3D foam printing with continuous solubilization.

a) Solubilization: the thermoplastic polymeric filament is impregnated inline with a liquid bath consisting of a mixture of a blowing and a non-blowing agent (Figure 2). The level of the bath and the concentration of the blowing agent in the liquid can be fixed at will. The fast and inline impregnation allows to tune the concentration of blowing agent while the object is printed. Indeed, the residence time of the filament in the bath ( $t_{sol}$ ) can be changed by varying the level of the liquid without the need of changing the printing speed. Furthermore, homogeneous or inhomogeneous concentration profiles of the blowing agent in the polymer can be achieved by tuning the residence time and liquid bath concentration. We remark that, for the sake of simplicity, the solubilization here presented is based on a liquid bath, nonetheless a solubilization stage with a gas can be implemented with a closed autoclave.

b) Desorption: when the filament exits from the bath, it enters in the desorption zone. Here, one can promote desorption so as to generate a blowing agent profile within the filament allowing to obtain controlled cellular morphologies in the foaming zone [17-20]. If this is not wanted, a negligible desorption might be also achieved. Desorption can be effectively controlled by modulating the residence time ( $t_{des}$ ) of the polymer in this zone.

c) Melting: as for the standard 3D printing, the impregnated filament is melted before accessing the nozzle [13]. Herein, the gas solubilized into the filament may affect the melting kinetics and form bubbles if the pressure is not sufficiently high.

d) Printing and foaming: the rapid pressure drop in the nozzle triggers bubble nucleation followed by bubble growth. Consequently, the printed strand reaches the desired density and morphology.

According to the units shown in Figure 1, we modified the 3D printer as reported in Figure 2. The bath is a simple beaker containing the blowing agent and is assembled on the printer structure before the extruder inlet. Figure 2b shows the details of the custom-made bath for the inline solubilization. In this work, we used acetone as the blowing agent for the inline impregnation of the PLA filament. The acetone was chosen because it is a good solvent for PLA [30] and it can be used for a fast inline impregnation of the filament.

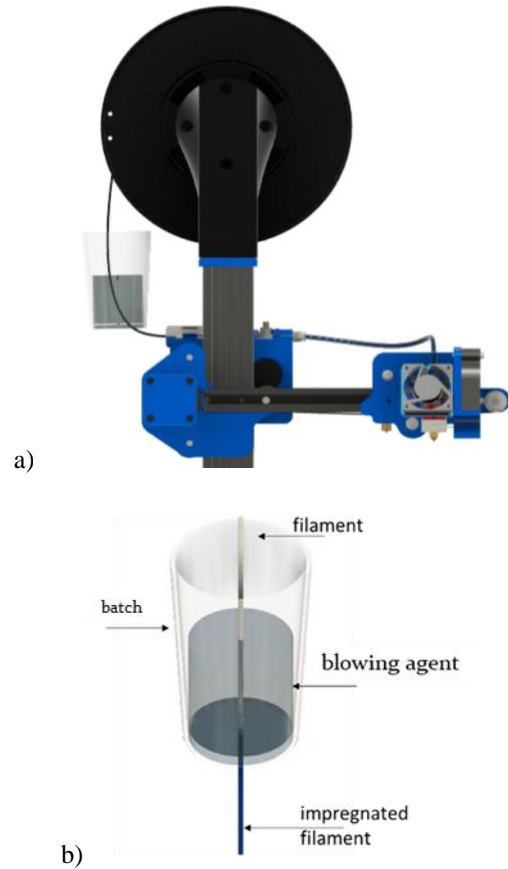


Figure 2: a) 3D printer modified for inline solubilization; b) custom-made bath for inline solubilization of the blowing agent into the filament.

The accessible ranges of the operating conditions are reported in Table 2. The nozzle temperature can be changed arbitrarily through the 3D printer software: conceptually, the lower limit is given by the melting temperature of the polymer (e.g., about 170°C for PLA) and the upper limit is the temperature at which the polymer starts to degrade (about 280°C for PLA). Hence, an experimental operating temperature range in between these two limits is considered. The software fixes the wall temperature of the brass nozzle in the 3D printer, which affects the melting kinetics of the filament and, hence, the instant at which the gas foaming starts. The foaming temperature,  $T_{foam}$ , is defined equal to the nozzle temperature. Also, the printing speed can be changed at will by the 3D printer software, which sets the polymer flow rate through the nozzle, thus the pressure drop that, in turn, can trigger the gas foaming. The largest speed is limited by slip at gears [17]. Finally,  $t_{sol}$  and  $t_{des}$  can be chosen based on the desired concentration profile of the blowing agent in the filament (as it is reported in the next section).  $t_{sol}$  can be tuned by changing the printing speed and/or the liquid height in the

beaker, whereas  $t_{des}$  can be tuned by changing the printing speed and/or the distance between the beaker and the melting zone. In this work, both  $t_{sol}$  and  $t_{des}$  range from 0.1 to 5 minutes, which are values comparable with the characteristic diffusion time of acetone in PLA at room pressure and temperature for the problem at hand.

In order to verify that the PLA strand reaches temperature conditions above its melting point before exiting the nozzle of the 3D printer, we performed a finite-element numerical simulation of the mass, momentum, and thermal energy transport phenomena occurring in it. A conservative verification of the achievement of the melting conditions was done by simulating the process in the “worst” case, namely, at the largest experimental printing speed and the lowest printing temperature.

Table 2: Process variables.

Temperature of nozzle [°C]	Printing speed [mm/s]	$t_{sol}$ [min]	$t_{des}$ [min]	Liquid height in beaker [mm]
180-260	1-50	0.1-5	0.1-5	2-500

### Foamed strands

With the proposed setup, we investigated the effects of the two most important process variables, i.e., the blowing agent concentration and the foaming temperature,  $T_{foam}$ , on the foam morphology and the density of strands.

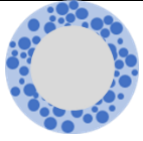
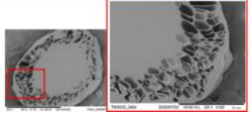
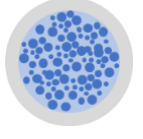
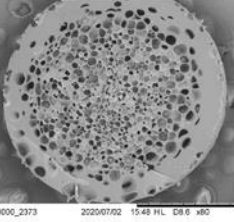

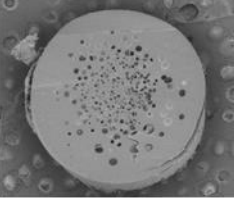

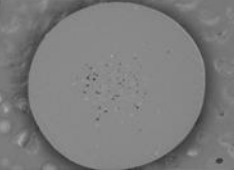
The average blowing agent concentration in the filament was varied by adjusting the solubilization time. In particular, a proper saturation is achieved when the acetone has diffused in the entire filament section. In order to quantify solubilization and desorption, two dimensionless times are defined:  $\bar{t}_{sol} = \frac{t_{sol}}{R^2/D}$  and  $\bar{t}_{des} = \frac{t_{des}}{R^2/D}$ , where  $R$  and  $D$  are the radius of the filament and the diffusivity of the blowing agent, respectively. So, the blowing agent impregnates the entire filament section when  $\bar{t}_{sol} > 1$ , the larger  $\bar{t}_{sol}$  the larger is its average concentration in the filament, indeed, we expect a concentration gradient across the filament section.

$D$  are the radius of the filament and the diffusivity of the blowing agent, respectively. So, the blowing agent impregnates the entire filament section when  $\bar{t}_{sol} > 1$ , the larger  $\bar{t}_{sol}$  the larger is its average concentration in the filament, indeed, we expect a concentration gradient across the filament section.

In Table 3, we present microfoamed strands with different blowing agent profiles produced at 210°C. With  $\bar{t}_{sol} < 1$  and  $\bar{t}_{des} \ll 1$ , the blowing agent penetrates only a small peripheral zone of the filament, thus the bubbles are expected to form only in such area. Indeed, a “ring” of bubbles is observed on the strand periphery, as shown on row 1 in Table 3. On the other hand, starting from a

impregnated filament, i.e.,  $\bar{t}_{sol} > 1$ ,  $\bar{t}_{des}$  can be varied to obtain microfoamed strands with a denser skin with respect to the bulk. On row 2 of Table 3, the cross section of the filament is shown for three values of  $\bar{t}_{des}$ . It is apparent that, as  $\bar{t}_{des}$  is increased, the bubbles are more localized in the core of the strand, whose expansion ratio correspondingly decreases.

Table 3: Different cell morphologies controlled by mass transport.

Conditions	Expected foam morphology	Observed foam morphology
$\bar{t}_{sol} < 1$ $\bar{t}_{des} \ll 1$		
$\bar{t}_{sol} \approx 6$ $\bar{t}_{des} \approx 0.1$		
$\bar{t}_{des} \approx 0.5$		
$\bar{t}_{des} \approx 1$		

$t_{des}$

### Conclusion

We reported the design of a novel continuous 3D printing process to produce thermoplastic polymeric foams with physical blowing agents solubilized inline. The resulting 3D printed foams were analyzed morphologically by SEM. The developed 3D foam printing technique allows

to fabricate polymeric cellular materials that, in turn, can be used to produce porous hierarchical structures in an economical and simple way. Needing only few grams of materials and few minutes for printing, our technique allows to save 40% of printed material and to quickly scan broad ranges of foaming conditions, e.g., foaming temperatures, pressure drop rates, etc. The possibility to form materials with the desired density through foaming combined to 3D printing opens up to the possibility to design new products with ad-hoc hierarchical structures.

## References

- [1] Redwood, Ben, Filemon Schffer, and Brian Garret. The 3D printing handbook: technologies, design and applications. 3D Hubs, 2017.
- [2] Berman B. 3-D printing: The new industrial revolution. *Business Horizons*. 2012; 55(2):155-62.
- [3] Stansbury JW, Idacavage MJ. 3D printing with polymers: Challenges among expanding options and opportunities. *Dental Materials*. 2016;32(1):54-64.
- [4] Wu P, Wang J, Wang X. A critical review of the use of 3-D printing in the construction industry. *Automation in Construction*. 2016; 68:21-31.
- [5] Okolieocha, C., Raps, D., Subramaniam, K., & Altstädt, V. (2015). Microcellular to nanocellular polymer foams: Progress (2004–2015) and future directions—A review. *European Polymer Journal*, 73, 500-519.
- [6] Lakes, Roderic. "Materials with structural hierarchy." *Nature* 361.6412 (1993): 511-515.
- [7] Grindy, Scott C., Robert Learsch, Davoud Mozhdehi, Jing Cheng, Devin G. Barrett, Zhibin Guan, Phillip B. Messersmith, and Niels Holten-Andersen. "Control of hierarchical polymer mechanics with bioinspired metal-coordination dynamics." *Nature materials* 14, no. 12 (2015): 1210-1216.
- [8] E. B. Duoss, T. H. Weisgraber, K. Hearon, C. Zhu, W. Small, T. R. Metz, J. J. Vericella, H. D. Barth, J. D. Kuntz, R. S. Maxwell, C. M. Spadaccini, *Adv. Funct. Mater.* 2014, 24, 4913.
- [9] Chen, Qiyi, Peng-Fei Cao, and Rigoberto C. Advincula. "Mechanically robust, ultraelastic hierarchical foam with tunable properties via 3D printing." *Advanced Functional Materials* 28.21 (2018): 1800631.
- [10] Zhou, C., Yang, K., Wang, K., Pei, X., Dong, Z., Hong, Y., & Zhang, X. (2016). Combination of fused deposition modeling and gas foaming technique to fabricated hierarchical macro/microporous polymer scaffolds. *Materials & Design*, 109, 415-424.
- [11] Minas, C., Carnelli, D., Tervoort, E., & Studart, A. R. (2016). 3D printing of emulsions and foams into hierarchical porous ceramics. *Advanced Materials*, 28(45), 9993-9999.
- [12] Chen, Qiang, and Nicola M. Pugno. "Bio-mimetic mechanisms of natural hierarchical materials: a review." *Journal of the mechanical behavior of biomedical materials* 19 (2013): 3-33.
- [13] Tammaro, D., Astarita, A., Di Maio, E., & Iannace, S. (2016). Polystyrene foaming at high pressure drop rates. *Industrial & Engineering Chemistry Research*, 55(19), 5696-5701.
- [14] Tammaro, Daniele, and Ernesto Di Maio. Early bubble coalescence in thermoplastic foaming. *Materials Letters* 228 (2018): 459-462.
- [15] Kiran, E. (2010). Foaming strategies for bioabsorbable polymers in supercritical fluid mixtures. Part I. Miscibility and foaming of poly (l-lactic acid) in carbon dioxide+ acetone binary fluid mixtures. *The Journal of Supercritical Fluids*, 54(3), 296-307.
- [16] Carbone, M. G. P., Tammaro, D., Manikas, A. C., Paterakis, G., Di Maio, E., & Galiotis, C. (2019). Wettability of graphene by molten polymers. *Polymer*, 180, 121708.
- [17] Osswald, Tim A., John Puentes, and Julian Kattinger. "Fused filament fabrication melting model." *Additive Manufacturing* 22 (2018): 51-59.
- [18] Lombardi, Lorenzo, and Daniele Tammaro. Effect of polymer swell in extrusion foaming of low-density polyethylene. *Physics of Fluids* 33.3 (2021): 033104.
- [19] Tammaro, D., Lombardi, L., Scherillo, G., Di Maio, E., Ahuja, N., & Mensitieri, G. (2021). Modelling Sorption Thermodynamics and Mass Transport of n-Hexane in a Propylene-Ethylene Elastomer. *Polymers*, 13(7), 1157.
- [20] Tammaro, D., Walker, C., Lombardi, L., & Trommsdorff, U. (2020). Effect of extrudate swell on extrusion foam of polyethylene terephthalate. *Journal of Cellular Plastics*, 0021955X20973599.